The use of pottery pans lowers the roasting temperature and gives the product a more favorable taste. This study uncovers the role of pottery particle on chlorogenic acid (CGA) decomposition during roasting process. This study aims to design pottery pans and the roasting process that optimize the CGA content and quality of the coffee using Indonesian traditional ceramics from Banyuwangi,East java named Kreweng. The pottery was ground to between 74–1000 μm before activation. The elemental, phase, and morphology characterization performs on the coffee bean. The morphology characteristic of the pottery observed further using digital imaging technique to unravel the pores and boundaries. The impact of the pottery usage for coffee roasting also tested through coffee product pH measurement. The pottery morphology determines coffee product acidity. The smaller the pottery catalyst particle size results in more acid coffee. The pore and grain boundary concentration increases as the particle size decreases. At the same time, the Si/Al ratio was higher at the smaller catalyst particle size with higher porosity, grain boundaries, and absorption. The porosity and defects reveal the negatively charged faces of the pottery crystal edges. The charged faces revealed due to the pottery crystal vibration in response to heat during roasting process. The effectiveness of surface contact is greater due to the distribution of negative charges around the pores that attract OH- side of CGA. This interaction traps hydrogen proton on catalyst conductive surface. As a result, the CGA decomposes into several groups of atoms and molecules including H_2 and CO_2. The interaction with the catalyst transforms the macronutrient into aliphatic acid. Therefore, roasting media with a higher Si/Al ratio at smaller particle sizes with high micropores will increase the rate of decomposition and the acidity of coffee products

Keywords: Si/Al ratio, Kreweng pottery, microstructure, CGA decomposition, coffee acidity

UDC 6.66.544.4
DOI: 10.15587/1729-4061.2022.260258

THE ANALYSIS OF SI/AL RATIO ON CGA DECOMPOSITION IN INDONESIAN TRADITIONAL KREWENG POTTERY COFFEE ROASTER TO MAXIMIZE COFFEE ACIDITY

Ikhwanul Qiram*
Master of Engineering, Senior Lecturer, Doctoral Candidate
Department of Mechanical Engineering
PGRI University Banyuwangi
Jl. Ikan Tongkol, 22, Kertosari, Kec. Banyuwangi, Kabupaten Banyuwangi, Jawa Timur, Indonesia 68416
Nurkholis Hamidi
Doctor of Engineering, Associate Professor*
Lilis Yuliati
Doctor of Engineering, Associate Professor*
Willy Satrio Nugroho
Doctor of Engineering
Department of Industrial Engineering
Brawijaya University
Ketawanggede, Kec. Lowokwaru, Kota Malang, Jawa Timur, Indonesia, 65145
I Nyoman Gede Wardana
Corresponding author
Doctor of Engineering, Professor*
E-mail: wardana@ub.ac.id
*Department of Mechanical Engineering
Brawijaya University
Ketawanggede, Kec. Lowokwaru, Kota Malang, Jawa Timur, Indonesia, 65145

Received date 17.06.2022
Accepted date 10.08.2022
Published date 31.08.2022

***How to Cite**: Qiram, I., Hamidi, N., Yuliati, L., Nugroho, W. S., Wardana, I. N. G. (2022). The analysis of Si/Al ratio on CGA decomposition in Indonesian traditional Kreweng pottery coffee roaster to maximize coffee acidity. Eastern-European Journal of Enterprise Technologies, 4 (2 (118)), 22–37. doi: https://doi.org/10.15587/1729-4061.2022.260258*

1. Introduction

Roasting is an important step in the development of specific organoleptic properties (aroma, taste and color) that underlie coffee quality [1]. During roasting, coffee beans will undergo physical and chemical changes due to an increase in temperature, time and roasting speed. Those changes affect the nutrition and the organoleptic properties of coffee. In this case, the selection of roasting media plays an important role in the phenomenon of heat transfer in coffee beans [2]. Hence, the evaluation of pottery material composition and morphology impact on coffee nutrition and organoleptic properties is necessary.

The organic chemical components in coffee have a dual role as nutrition and organoleptic properties determina-

tion factor. Green coffee beans contain many chemical components including caffeine, chlorogenic acid (CGA), trigonelline, carbohydrates, fats, amino acids, organic acids, volatile aromas, and minerals [3]. CGA as the main phytonutrient of coffee is an active polyphenol antioxidant that has chemo-preventive ability, antibacterial, antifungal, and has diabetes prevention role [4]. CGA is also responsible for the acidity and bitterness of roasted products which were the factors to assess the quality of coffee [5]. The CGA content in Robusta coffee beans is higher around 7.0–4.0 % (dm) and up to 9.0 % on green coffee beans [6]. Due to its natural occurrence, CGA is utilized as a unique biomarker to identify the quality of roasted coffee products [1]. Even though, the roasting process reduced the amount of antioxidant content in coffee including the CGA. Hence, The darker the color of the roasted coffee beans, the lower the CGA content [7]. This is consistent with the findings in several studies which classify CGA as heat-reactive phenolic compound based on its thermal oxidation and square-wave voltammetry (SWV) data [8]. SWV results unveil the chemical structure and electronic properties determine CGA reactivity. Especially, the electron donating effect of the -OH and -CH=CH- groups, and the strong electron-withdrawing effect of the ester group (-COOR) [9]. Therefore, it is important to carry out the evaluation of coffee roaster and coffee beans material interaction.

The coffee roaster material defines the final organic composition according to its heat-transfer mechanism. Ground coffee products that roasted using a clay-based skillet were preferable to a metal pan roasted coffee [1]. Not limited to coffee, the use of clay-based inorganic catalysts has been commonly used in various food processing industries. Clay has ecofriendly, economical, recyclable and non-corrosive properties so it is more efficient when used in organic reactions [10]. Alongside to that, clay is a ceramic based material that arranged by cubical crystal lattice. The crystal lattice was formed by the ionic bonds between the metal core and non-metal face [11]. Unlike the metal cubical crystal lattice, the ionic bonded cubical lattice is more rigid. This was due to non-symmetric electrostatic interaction between heavier atoms with lighter atoms that prevents the core and the face from displacement. Historically, Clay has been the main material for making pottery, porcelain and other necessities for thousands of years [12]. In general, clay contains silica compounds, clay minerals and humus [13]. The minerals in clay make a major contribution as a chemical absorber material with various types of interactions due to its horizontal sheet structure which is hydrophobic on one surface and hydrophilic on the other.

Pottery (pottery) is a traditional clay-based ceramic with a simple burning technique and functions as household utensils. The quality of pottery is influenced by the fraction of the constituent materials and manufacturing techniques [12]. Pottery is a type of porous ceramic, where the formation of pores is caused by the process of compacting the material and refining the clay grains so that the clay pores are closer together. The density of the clay pores will suppress dry shrinkage during the calcination process, thereby triggering changes in the microstructure such as grain growth, pore shrinkage and shrinkage [14]. In modern ceramic technology, modification of the ceramic constituent mixture is often carried out to obtain the desired product characteristics. As well as the addition of SiO_2 which can form a liquid phase so as to allow improved densification of alumina ceramics [15]. Recently, the synthetic or natural inorganic porous materials utilization and development such as zeolites, pillared clays, and phosphate derivatives as ion exchangers is getting a lot of attention. These porous materials have high chemical stability, rigidity and heat stability making them suitable for almost all ion exchange applications [16]. Consequently, pottery material showing superior, versatile and modifiable properties to be used as coffee roasting catalyst.

Many studies and articles have focused on the effects caused by the use of modern roasting machines, causing the Kreweng pan has not been widely studied and known by the wider community about its effect on the taste of the coffee product obtained. Meanwhile, for most people in the local coffee industry, such as in Indonesia, modern roasters are relatively expensive and take a long time to learn how to use them. Therefore, the findings of the investigation will provide technical information that leads to technological improvements and improve the quality of local coffee products.

2. Literature review and problem statement

The coffee sensory and organoleptic properties are mostly determined parametrically. The multi-study review of coffee roasting processes show bean color and roasting time are the sensory properties marker parameters [17]. The phase of a roasting duration can be classified to “time to first crack” In which the duration of steam pressure buildup to crack the coffee bean and “the development time” as the time to develop sensory and organoleptic properties of a coffee measured from the “time to first crack” to the end of roasting process [18] in general, more favorable sensory characteristics. After roasting, analytical methods are required to differentiate species. Blends with different proportions of arabica/robusta coffees, roasted at three degrees were studied. Color parameters and the levels of chlorogenic (5-CQA. During the development time, the chemical composition shift is occurring. Another report suggest that the control on coffee development time is more important than time to first crack [19]. The duration of chemical composition shift controls the taste and aroma of the coffee. The fast roasting time increases fruitiness, sweetness and acidity of coffee product. Meanwhile, longer development time generates roasted, nutty+chocolate, and bitter taste. However, the chemical reaction during the chemical shift under a certain development time is depends on the roaster material exposure.

The other parameter to control coffee quality is the roasting temperatures. Long roasting process with constant temperature so called baking triggers chemical shift [20]. However, the phenol content is largely depend on the optimal roasting time–temperature profile [21]. Alongside to that, the taste of a coffee is fully depend on the successful palmitic acid decomposition to oleic, linoleic, linolenic, and arachidonic acid which depend only on temperature profile [22]. Even though, every heating

process is unique. Heating coffee with microwave increases its oil content by 27.5 %, reduces the phenolic content by 16.6 %, and reduces 37.63 %the total antioxidant [23]. This because, the microwave radiation is not transferring heat from a heat source to an object instead it is vibrates the molecules to intrinsically heating itself [24]. Therefore, the heating dynamics of a coffee bean roasting determine the end product quality. This study evaluates the dynamics of roaster material interaction with coffee bean content.The active inorganic content of many potteries is an alumino-silicate ($nM_2O.Al_2O_3.xSiO_2.yH_2O$) [25]. In general, ceramics have a surface structure composed of sialate monomer units (Si-O-Al-O) in the form of a negatively charged network or dominated by electric charge carriers (holes) that allow ion mobility, and affect the conductivity properties of the material [26]. Through the polycondensation process, the monomers in the silicate solution will be arranged into alumino-silicate anions which have a main chain called polysalat. Polysalat is a negatively charged network composed of $[SiO4]^{4-}$ and $[AlO4]^{5-}$ tetrahedral which are connected to each other through covalent bonds and cations from alkali metals such as Na^+, K^+, Li^+, Ca^{2+}, and Ba^{2+} that fill into the tissue cavities to balance the negative charge of Al^{3+} in tetrahedral coordination [26]. The properties of alumino-silicate catalysts are generally based on the Si/Al ratio and the type of activation of the material. The difference in the Si/Al ratio has an effect on the crystallinity or amorphous nature of the ceramic material. The presence of amorphous silica in ceramics increases the adsorption ability and high selectivity. However, to obtain superior alumino-silicate catalyst capabilities, special treatment and high production costs are required [27]. For this reason, mechanical milling techniques are often chosen to produce different amorphous phase ceramics, intermetallic compounds, solid solutions, or nanocrystaline alloys [28]. Consequent to that reason, this study employs mechanically milled Banyuwangi, Indonesia traditional pottery as to develop the coffee roaster. Therefore, this study focuses on the material interaction of a pottery to develop a coffee roaster that maximizes the acidity of the coffee product.

Previous studies mainly focus on parametrical control of the coffee roasting process to obtain coffee product with better quality. The Si/Al content in kreweng pottery offers advantages that allow roasting operations to be carried out at low temperatures making it suitable for materials that are not heat-resistant such as coffee. Optimization of material by mechanically milled to increase the selectivity of the material surface. The ionic interaction of alumino-silicate with coffee beans is discussed in this study. The discussion about the effect of aluminum and silicon ratio impact on kinetics due to heating on CGA transformation to aliphatic acid is also present. Therefore, the coffee acidity can be maximized through alumino-silicate content ratio control.

3. The aim and objectives of the study

The aim of this study is to determine the optimal configuration of alumino-silicate content ratio in a Banyuwangi, Indonesia traditional pottery upon maximizing the coffee acidity. To achieve the aim, the following objectives were accomplished:

– to investigate the effect of alumino-silicate ratio on coffee roasting temperature profile;

– to explore the pottery characteristics on various alumino-silicate content ratio;

– to view the impact of alumino-silicate content ratio on coffee product properties.

4. Materials and methods

This study uses pottery as an inorganic catalyst which is believed to have the main constituent element alumino-silicate (Si/Al). This research uses pottery as an inorganic catalyst which is believed to have the main constituent elements of alumino-silicate (Si/Al). Alumina-silicate in pottery has a negatively charged network structure that can affect heat transfer on the surface of the material. Modifying the surface of the crystalline phase to be amorphous, is expected to give a greater increase in contact stress. This increase is related to the ability of the alumino-silicate absorption peak to attract some of the hydroxyl [OH-] in CGA in the coffee roasting process. The electron affinity that occurs has an impact on the rate of decomposition of the material which is characterized by changes in the water content and acidity of the final product.

The pottery media was obtained from the brick and pottery industry in Kedung Gebang Village, Tegal Delimo District, Banyuwangi Regency, East Java, Indonesia. The pottery media was a traditional ceramics from Banyuwangi,Indonesia named Kreweng. The media was processed using a ball mill machine type SS 10-35, 220 V, 80 rpm for 60 minutes. The earthenware powder was sieved using 18, 60 and 200 wire mesh to obtain catalyst particles at sizes 250 μm<(P_1)<1000 μm, 177 μm<(P_2)<250 μm, and (P_3)>74 μm. While the Green Bean (GB) material used is robusta coffee (*Coffea canephora*) medium type with a moisture content of about 12–14 % (bb) obtained from the Kampong Kopi Lerek Gombengsari (*Kopilego*) Plantation, Banyuwangi, East Java, Indonesia.

Characteristic morphology of pottery catalysts sample and coffee products were observed by FEI inspect-S50, Scanning Electron Microscope (SEM) in high vacuum mode and energy dispersive x-ray (EDX). The characteristics of the wavelengths that absorbed by the catalyst and the GB were determined using UV-Vis Spectrophotometry. The spectrophotometer was UV-Vis 1601 Spectrophotometer (Shimadzu, Japan). The wavelength was emitted in the range of 200–800 nm. The UV-Vis sample was prior-activated catalyst powder with particle size ranging between 74–1000 μm. In addition, GB was also analysed with IR-Prestige 21, Fourier Transform Infrared (FTIR) (Shimadzu, Japan). FTIR measures the range of wavelengths in the infrared region absorbed by the GB through the application of infrared radiation to a sample of a material. The sample absorbance of infrared light energy at various wavelengths is measured to determine the molecular composition and structure of the material. XRD phase analysis of the catalyst was carried out using a PanAnalytical type E'Xpert: Pro in Bragg-Brentano geometry using a Cu anode with a Kα source (1.5405) and a Ni Kβ filter. Scanned Bragg angle is 10–90° with 0.0010° in 0.7 seconds for each step. The gap used is a fixed divergence gap of 1.52 mm and a receiving gap of 0.10 mm:

$$\varphi = \frac{A_T}{A_{TP}} \times 100\,\%. \quad (1)$$

The surface area, pores, and the catalyst pore size were analyzed using ImageJ software. This software plots the surface of an 8-bit image based on the byte pattern of the pixel brightness. A byte is 256 bit ranging from 0 to 255, the higher the byte the brighter the pattern [29]. The total surface area of the analyzed sample (A_T) and the total analyzed pore area of the sample (A_{TP}) data were used to estimate the porosity based on image obtained through (1). Alongside to that, the pore identification by digital imaging also performed through image-thresholding technique using 50 by 50 brightness to contrast histogram.

The roasted coffee products physical characteristics, water content and acidity (pH) were reviewed before and after treatment. The bean physical characteristic were the seed density analysis before and after the roasting process and water content testing using HB43-S moisturemeter. The Moisture Analyzer was focused on measuring the moisture content of the sample before and after roasting. The acidity test was performed on each coffee roasting step. The steps were start with grinding the coffee beans with a grinder, and then 2.25 grams of coffee powder was mixed with 50 ml of distilled water which was heated and then cooled to room temperature. The coffee solution was separated from the precipitate by filtering through Whatman No. 1 filter paper. Acidity level was measured using a pH analyzer (Model Pocket-sized pH meter KL-009A) [30].

The arrangement of the roaster measurement setup is as shown in Fig. 1. The roasting process was carried out in a cylindrical furnace with a total volume of 331.96 cm^3 made of 18/8 Stainlees Steel plate with a thickness of 0.4 mm. The inner wall of the tube was insulated using wood charcoal carbon powder 1 mm thick to avoid the radiation effect of the furnace material during roasting. This performed by considering the remarkable dielectric permittivity, dielectric loss angle tangent, and microwave response properties that possess by activated carbon [31].

The temperature of the catalyst powder and coffee beans were measured using K-Type thermocouple made of Chromel (Ni-Cr alloy) with a temperature range from 200 °C to 1200 °C. Each sensor port was connected to the notebook via the Arduino Uno R3 microcontroller. The roasting stage was carried out by heating 100 g of powder in a furnace using an electric heater (300–600 W, AC 220 V). Powder heating was carried out until it reaches a temperature of 200 °C and then followed by inserting 10 g of coffee beans into the heated powder. In 20 minutes roasting duration, the temperature data of the powder (T1) and coffee beans (T2) were recorded at intervals of 10 seconds.

5. Results of the alumino-silicate content ratio characterization and roasting evaluation

5. 1. Effect of alumino-silicate content on catalyst temperature profile

The temperature profile of the coffee bean roasting has enabled to declassify the heating rate dynamics of each roasting treatment to obtain ideal temperature. The ideal temperature for roasting is 200 °C. Fig. 2, *a* shows the heating rate of the electric heater used as a roasting energy source is 7.73 °C/minute or 0.13 °C/second. Fig. 2, *b* shows the heating rate of each catalyst and electric heater in 30 minutes of roasting. In Fig. 2, *b* the region of the chart can be dissected into two parts.

The first part at the top of the chart represents the heating rate of the electric heater and P_1 catalyst. In this part, the heating process was started by linear incremental pattern that followed by small logarithmic incremental, and logarithmic decrement pattern. The P_1 catalyst has shown slower heating process with lower peak temperature compared to electric heater. The second part located under the first part, represents the heating rate of P_2 and P_3 catalyst. Both catalysts heating rate was exponential with power factor in between 1.0 and 2.0. Fig. 2, *b* also shows the P_1 catalyst reach the ideal temperature in 32 minutes, P_2 in 30 minutes and P_3 in 25 minutes. This indicates that particle size affects the heat absorption and transmittance mechanism of each catalyst.

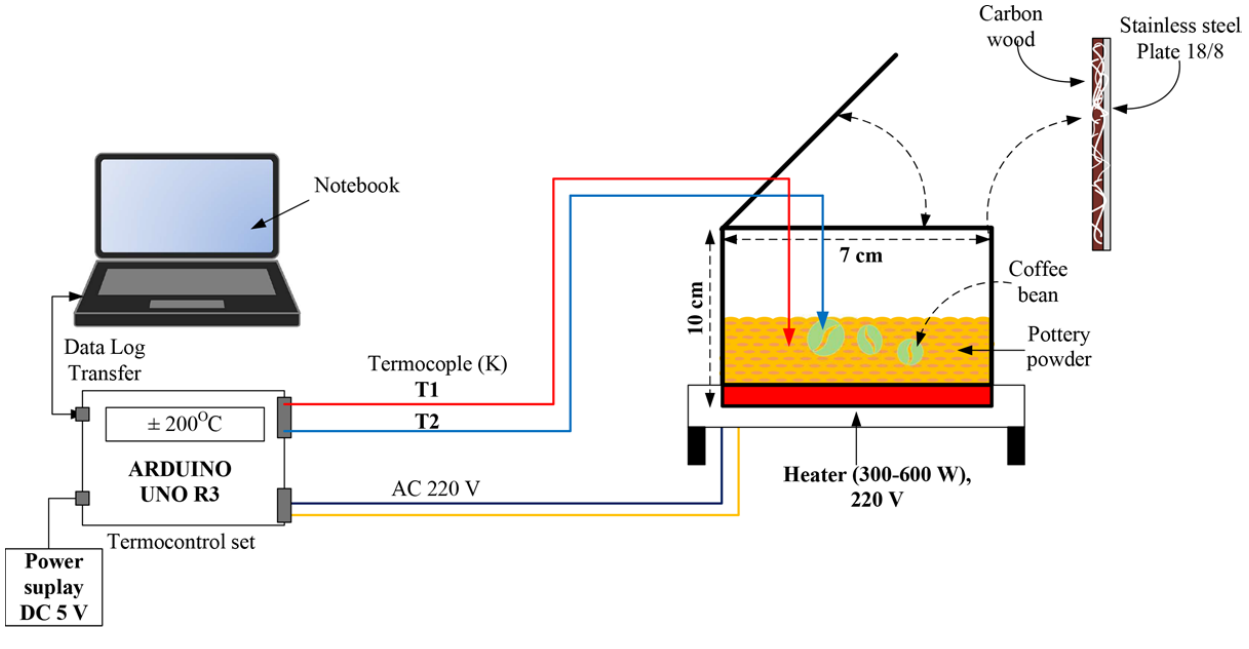

Fig. 1. Roaster Measurement Setup

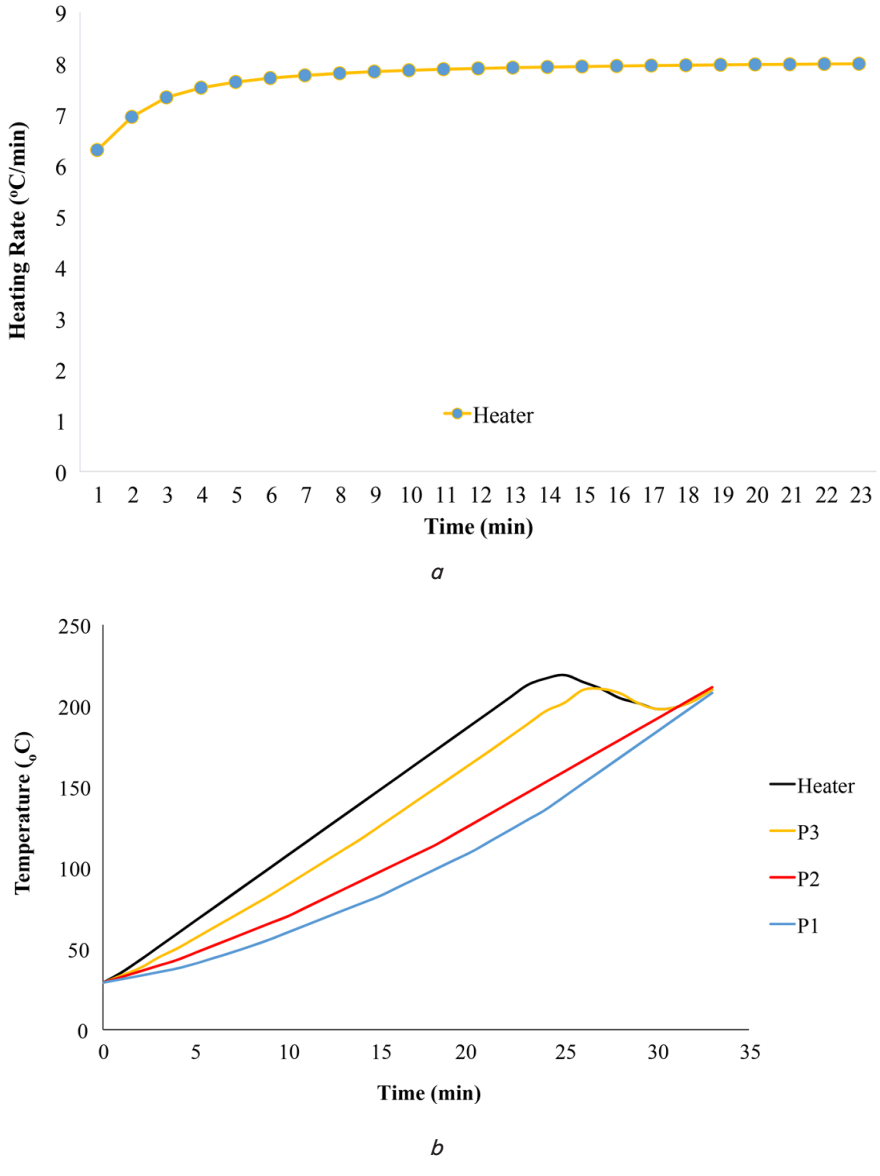

Fig. 2. Temperature profile: *a* — heating rate of electric heater; *b* — comparison of electric heater temperature to variation of pottery catalyst size

5. 2. Impact of alumino-silicate on pottery catalyst characteristics

The UV-Vis spectra of each catalyst have help to identify the catalyst structure, compounds, and predict the reactivity of each catalyst. As shown in Fig. 3, the light absorbance peak of each test specimen has an absorption peak at a wavelength of 320 nm due to the presence of alumino-silicate. This condition indicates that the light absorbance peak is related to the electron absorbance on the surface structure of the catalyst. P_1 and P_2 catalysts have a lower absorption of 1 K/M due to the larger particle size so that the contact surface area were small. While the P_3 catalyst has a maximum absorption at 1.8 K/M due to the smaller particle size. In addition to that, the increasing numbers of pores on the catalyst surface has triggers more significant surface response. In accordance with structural identification, the UV-Vis also can track energy level of each catalyst. The high light absorbance of P_3 in short wavelength region indicating its compounds were less reactive to longer wavelength. Hence, the energy level of P_1 and P_2 were higher than P_3 which depicts the reactivity with lower energy.

The additional elemental analysis through FTIR was carried out to detect the functional groups that existed in the catalyst. Fig. 4 shows the characteristics of the pottery catalyst sample in the absorption region at a wave number of about 462 cm^{-1} which is the absorption of Si-O vibrations, at a wave number of 536.2 cm^{-1} is a stretching vibration of Si-O-Al, at a wave number of 1635.02 cm^{-1} is bending vibration –OH, 3447.8 cm^{-1} is stretching vibration –OH, and at wave number 3629.35 cm^{-1} is stretching vibration of –OH. These numbers are identical to the spectra of clay as the main composition of pottery materials [32]. FTIR test results have confirmed the presence of alumino-silicate in pottery catalysts which have the potential as inorganic catalysts in the coffee roasting process.

XRD phase analysis was carried out to confirm the crystallographic properties of the P_1, P_2 and P_3 pottery

catalysts. The wider XRD peaks indicate more X-rays are reflected to the detector at various contact angles [33]. Peak intensity shows level of crystallinity density on the catalyst surface [26]. Fig. 5, *a* shows that catalyst P_1 has a peak intensity of 3400 a.u at an angle of 2θ (°) of 27.79°, Fig. 5, *b* catalyst P_2 with an intensity peak of 3500 a.u at an angle of 2θ (°) of 28.02°, while P_3 in Fig. 5, *c* has a peak intensity of 4500 a.u at an angle of 2θ (°) of 27.78°. The x-ray diffraction pattern similarity of Fig. 5, *a–c* indicates the crystal structure of P_1, P_2, and P_3 catalysts were in equal phase. The results show that the material phase was consists of amorphous crystal and regular crystal materials.

The experimental results and the characterization results were connectively inform the underlying mechanism of the pottery catalyst. Intensity difference on each catalyst triggered by changes in particle size due to the milling process which is accompanied by an increase in defects that cause amorphous properties of the catalyst material. The amorphous nature of the pottery surface was also caused by the Si/Al ratio so that there is a shift in the absorption wavenumber to a higher number in the FTIR spectra shown in Fig. 4. In this situation, the pores in the pottery will modify the surface interaction forces with the coffee molecules. The results inferred that the kinetics of the catalysts was determined by its structural properties (grain size, pore density on the surface, etc) and the alumino-silicate composition. There was an indication that the structure of the catalyst may define the catalyst kinetics. For example, the pores in the pottery may modify the surface interaction forces with the coffee molecules due to the increasing surface area of reaction.

Morphological analysis was carried out to define surface characteristics as the basis to predicts surface kinetics of the catalyst. Visually it appears that the pottery catalyst has various surface characteristics (Fig. 6). P_1 catalyst shows a surface with a lump-like shape, while P_2 and P_3 appear to have dominant pore growth along with the smaller particle size. Fig. 6 also provides a pore identification results through image-thresholding technique. The black colored segments were represents the surface portion that does not holding incidence electrons and not covered by secondary emission light. Therefore, the black colored segment referred to the pores and grain boundaries. Based on the visualization of threshold images, the P_3 catalyst has more pores than P_2 and P_2 has more pores than P_1 (Fig. 6). The grain boundaries also do not exist on P_1 catalyst surface.

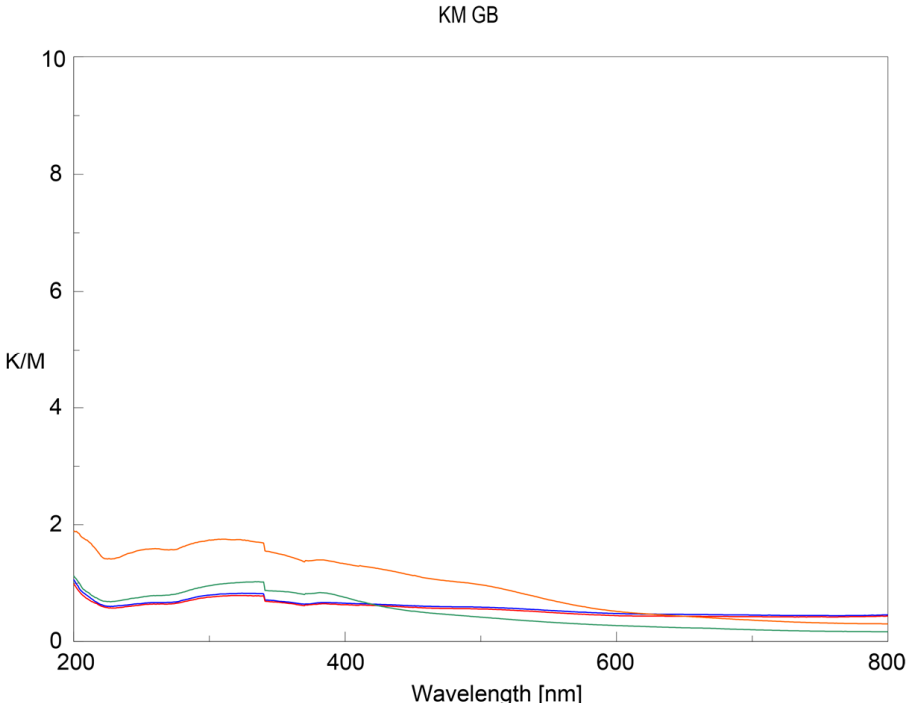

Fig. 3. UV-Vis spectra of pottery catalysts

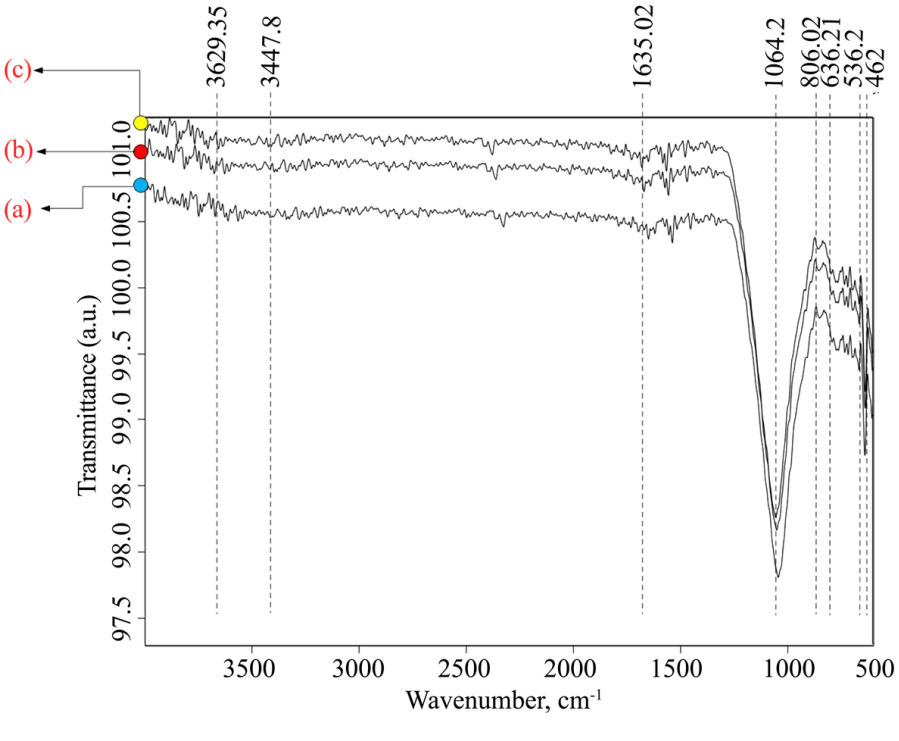

Fig. 4. FTIR test results of pottery catalysts: *a* – P_1; *b* – P_2; *c* – P_3

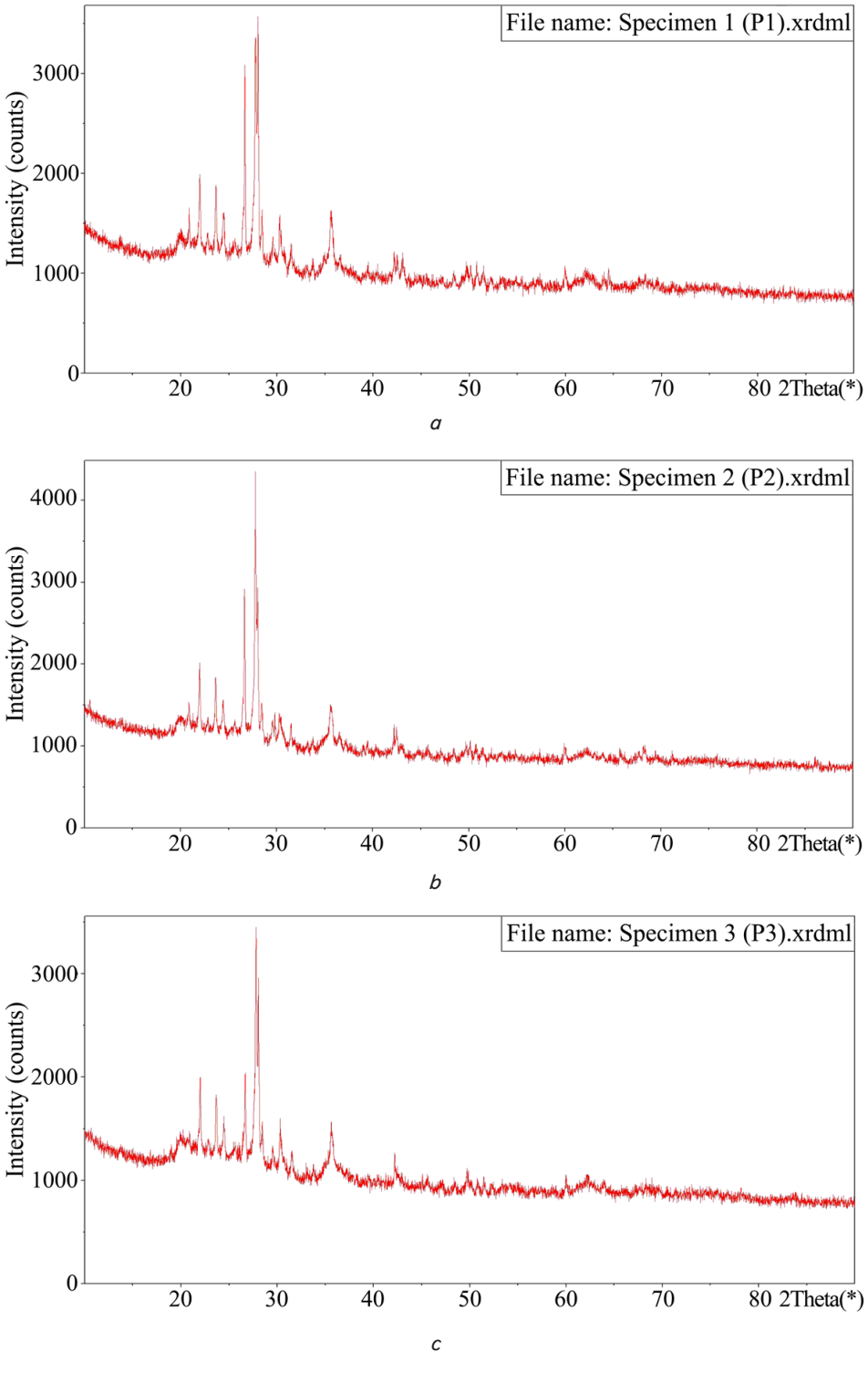

Fig. 5. XRD pattern of each pottery catalyst *a* – P_1; *b* – P_2; *c* – P_3

Further pore identification using quantitative technique by employing equation 1 also performed. The particle porosity calculation were tabulated in Table 1. The measurement results show that the smaller the catalyst particle size, the higher the percentage of micropores. This condition is influenced by the crystal size, where the larger the Si/Al ratio, the smaller the crystal size [34]. The milling process makes the crystal lattice defect due to the collision of the balls which increases the surface porosity as shown in Fig. 6.

Table 1

Porosity value in *Image-J* software analysis

Label of sample	Particle diameter (μm)	Total pores	Area (%)		
			Macros	Meso	Micro
P_1	646,855	162	11.73	29.63	58.64
P_2	191.40	659	7.59	28.53	63.38
P_3	39.97	767	9.39	20.08	70.53

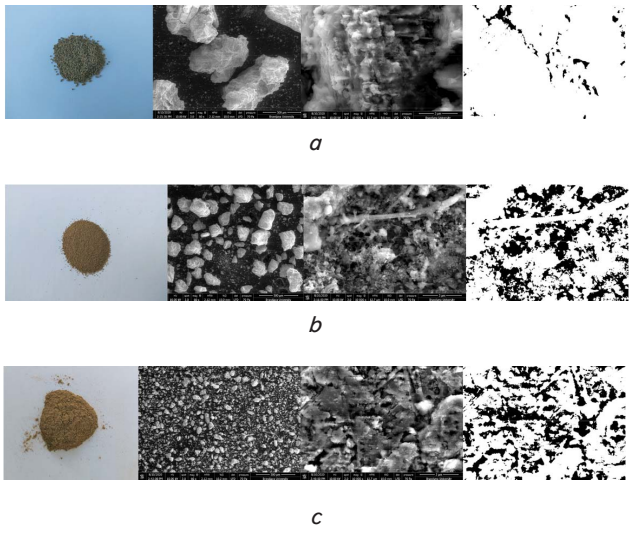

Fig. 6. Image-J of pottery catalyst *a* — P_1; *b* — P_2; *c* — P_3

The macro-pores observation coupled by surface plot of SEM image found the surface charge arrangement around the pores. In Fig. 7, *a* the macro-pores were clearly visible as the dark region. The targeted pore inside the red box has been used to analyze the surface plot. This due to its located near to 50th percentile of overall image brightness threshold. As a result, the plot in Fig. 7, *b* was generated according to it. The surface plot around the pore does not showing high brightness region. Surface brightness can indicate the surface charge of the SEM images [35]. The application of surface charge analysis has been implemented to observe interchanging surface polarity around macro and meso-pores [36]. Consequently, the dark surface brightness indicates the negative surface charge. Thus, the alumino-silicate presence around the pores can be confirmed.

The EDX results of pottery catalysts sample show the different atomic composition of its surface. The results were depicted in Fig. 8, *a–c* for each catalyst P_1, P_2, and P_3 respectively. Based on the resulting spectra, it can be seen that catalysts with different sizes have different percentages of Si/Al. However, the Si/Al ratio always maintained throughout all samples. Si atoms weight % were always narrowly more abundance than Al atoms on the catalysts surface (Table 2). This consistent with the detection of Si-O stretch on FTIR results (Fig. 4). The findings of abundance oxygen, some metal elements, and Si on catalyst surface related to the possibility of metal oxide and silicon oxide formation. Even though, the possibility was restricted by the cubical crystal lattice of clay. The only possible scenario for the metal oxide and silicon oxide formation is by crystal defect exploitation. Here, the grain boundaries and pores on pottery catalyst samples crystal were present on whole samples. Thus, the defective crystal promotes the metal-oxide and silicon-oxide formation.

Further elemental analysis based on atomic weight that decomposes each catalyst has unveiled the conductive surface formation. The Ti element was not present on P_2, insignificantly present on P_1, and present on P_3 (Table 2). The presence of Ti along with oxygen indicates the formation of Titanium-oxide (TiO_2). The Titanium-oxide may reside from rutile ore mineral from the clay source. The presence of Fe and Ti atoms also consistent with the XRD results that show ilmentite peak. Hence, there is high probability for Ti and Fe oxides formation. Those metal-oxides are useful in ion transport especially as cations transporter in electrochemical system [37]. Also, the significant amounts of Fe on catalyst samples enable the alteration of pottery catalyst conductivity.

Table 2

Chemical composition of pottery catalyst

Element	Weight %		
	P_1	P_2	P_3
C	33.53	19.39	15.4
O	37.53	39.28	36.89
Si	9.94	9.98	5.23
Fe	9.28	23.31	28.61
Ti	1.03	0	9.45
Mg	0.37	0.88	0.62
Al	7.22	5.4	3.35
Ca	1.11	0.82	0.45

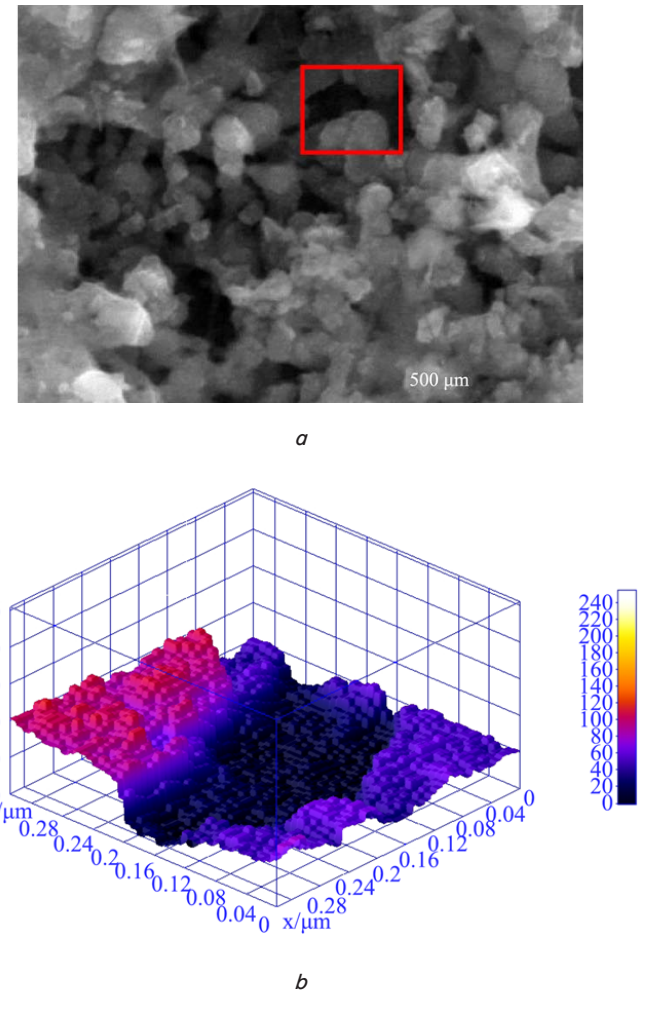

Fig. 7. Observation of pottery catalyst pores: *a* — Surface area to be plotted; *b* — 3D surface plot of catalyst using ImageJ

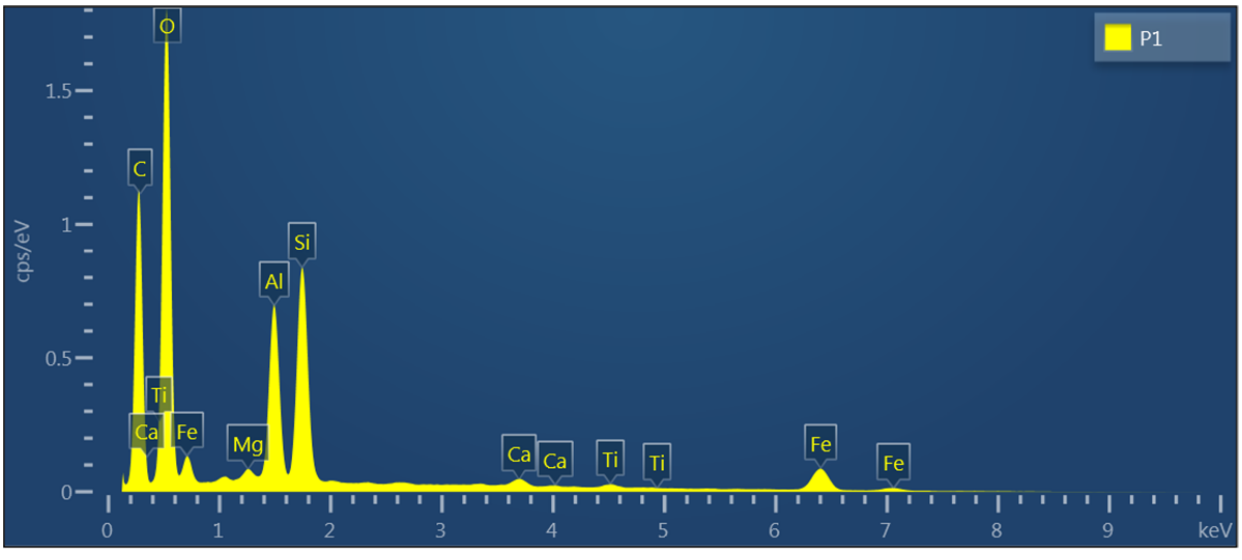

a

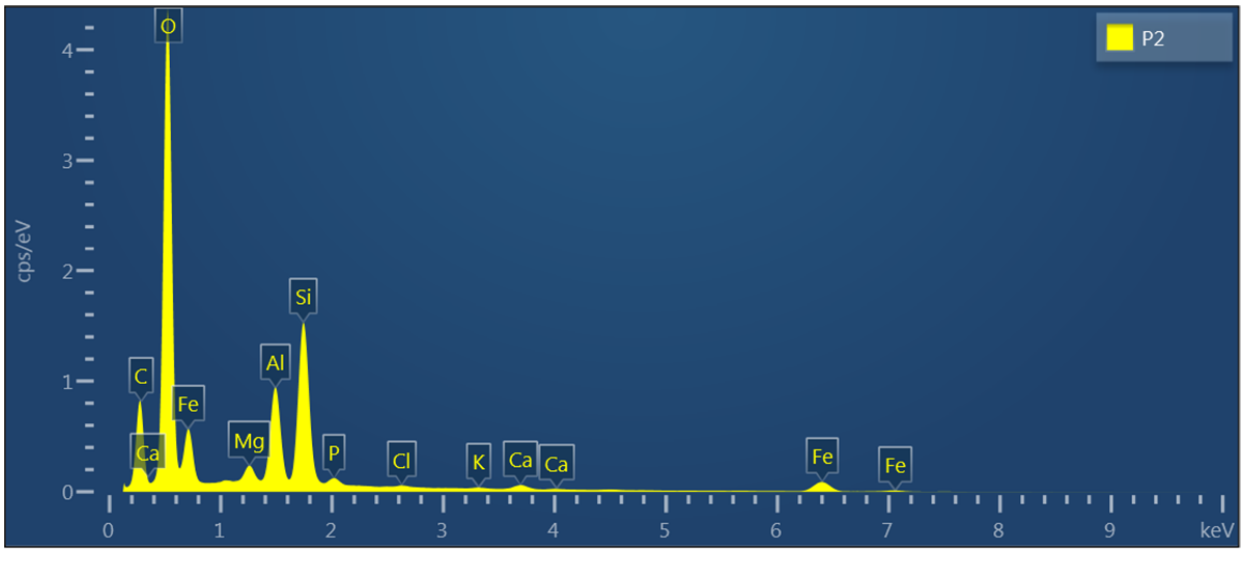

b

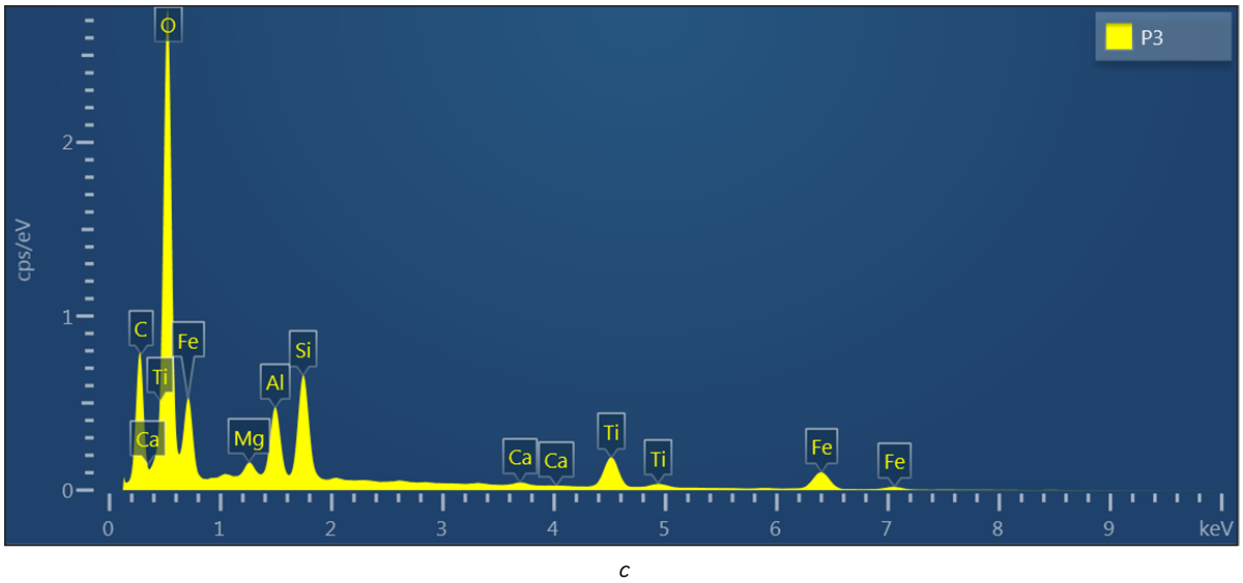

c

Fig. 8. EDX Spectra of pottery catalysts: *a* – P_1; *b* – P_2; *c* – P_3

5. 3. Alumino-silicate ratio impact on coffee product properties

The morphology characterization of GB sample was also performed to gain full mechanistic understanding of the catalyst and substrate interactions. The SEM image of GB in Fig. 9, *a* depicts the irregular grain morphology. The consequence of this will be the non-homogeny surface reaction occurrence due to the heterogenic substrate surface area. However, further surface characteristic identification on the outermost grain in Fig. 9, *a* (inside red rectangle) has reveal the surface charge homogeneity as shown in Fig. 9, *b*. According to the surface charge analysis principle, the surface tends to be brighter when it able to hold electrons [35]. Hence, the surface emits photons following the quantum electrodynamics (QED) principle due to the fallback electron on sample surface [38]. Previous study on organic electrocatalyst development has indicating the bright surface of SEM images on the flat contour as the polar positive surface [39]. Therefore, the GB surface was covered by positively charged substances. The phenolic antioxidant content has positively charged methoxyphenyl arrangement that also contribute to positive polarity of turmeric protein complex [40]. Therefore, the positive surface of GB was due to its high phenolic antioxidant content. The generalization can be made from this finding is the reaction of GB surface with pottery catalyst will cause molecular structure deformation of GB through electrostatic interaction.

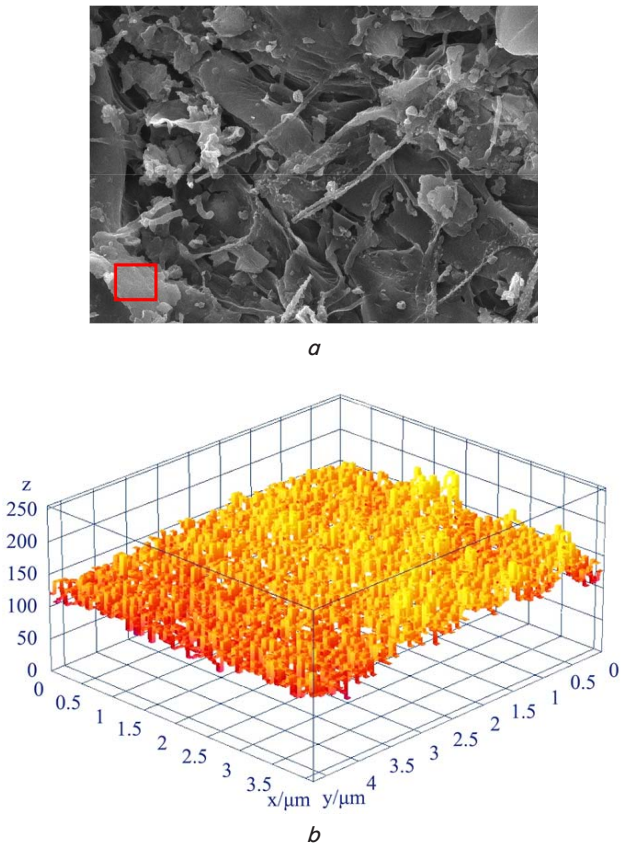

Fig. 9. Observation of green coffee bean surface: *a* — chosen surface area for 3D plot; *b* — 3D surface plot of coffee beans

Fig. 10 shows the coffee roasting performance with various pottery catalyst. It is shown that the yellow line (K_3) is the temperature condition of coffee roasted using P_3 catalyst, red color (K_2) indicates coffee roasting with P_2 catalyst and blue (K_1) is coffee roasting using P_1 catalyst. In the case of K_1 roasting, the temperature of the beans is much lower than the catalyst temperature. The highest bean temperature was only 119 °C which lasts until the end of the process (600 sec). The low porosity of P_1 causes a decrease in the ability of the catalyst to transmit heat to the coffee beans. This can be linked to the UV-V is light absorption of each catalyst. The low surface porosity of the catalyst greatly affects the intensity of energy absorption of the catalyst as shown in Fig. 3. P_1 and P_2 catalysts have lower absorption (1 K/M) than P_3 (2 K/M) due to their larger grain size so that the contact surface area is very small. This connectivity has inferred that the adsorption of the catalyst surface active site can be characterized through energy release in the form of heat. Therefore, temperature profiles represent the performance of pottery catalysts in coffee bean roasting.

Fig. 11 shows the results of the FTIR spectra of Green Bean, the product roasted with P_1–P_3 catalyst and the product sample from conventional roasting. The FTIR test in this case aims to identify changes in product functional groups in various roasting operating conditions. The test results showed absorption data at 1033.07 cm^{-1} (CO), 1157.99 cm^{-1} (C=CH), 1647.71 cm^{-1} (C=C aromatic), 1744.31 cm^{-1} (C=O stretch), 3345.83 cm^{-1} (width, OH stretch). Within those regions, the coffee products contain less aromatic C=C and not showing free OH stretch. The loss of free OH stretch can be occurred due to the carbohydrate heating process. The use of catalysts has changed the mineral composition of the coffee products which can be seen from the right hand side (RHS) of the FTIR spectra. This related to the variation of mineral content of the pottery catalysts. The high Fe and Ti P_3 catalyst has stronger peak on 634.42 cm^{-1} compared to other peaks (Fig. 11, *d*). The alumino-silicate related functional groups were not detected which indicating no degradation occurrence of the pottery catalysts. However, the CGA content change is untraceable because the main atomic compositions of GBA are [CH] alkane groups, C=C groups, and phenolic [OH] groups. In addition to that, other coffee antioxidants such as hydroquinone have similar functional groups. This may cause FTIR spectrum to overlap which makes the source molecules of each functional group undistinguishable. On the other hand, the transmittance energy differences were due to the different composition of the detected functional groups that affects the surface contact energy of the coffee beans with the pores of the pottery catalyst. Consequently, the decomposition rate can be different according to the operating conditions.

The acidity level comparison in Fig. 12 shows the change in the acidity value of green coffee beans (GB) with a value of 4.98 to become 4.67 with P_1 catalyst roasting indicated by K_1, P_2 catalyst roasting indicated by K_2 and to 3.70 with P_3 catalyst roasting indicated by K_3. The results of pottery catalyst roasting showed the higher the acidity level along with the smaller catalyst particle size. This was caused by the decomposition of sucrose, glucose and fructose compounds to form aliphatic acids compounds. The surface area of the catalysts has shown to be involved in resulting aliphatic acid concentration. This condition was triggered by the adsorption energy of the catalyst on the surface of the coffee beans which is simultaneously characterized by an increase in the temperature of the beans as shown in Fig. 9.

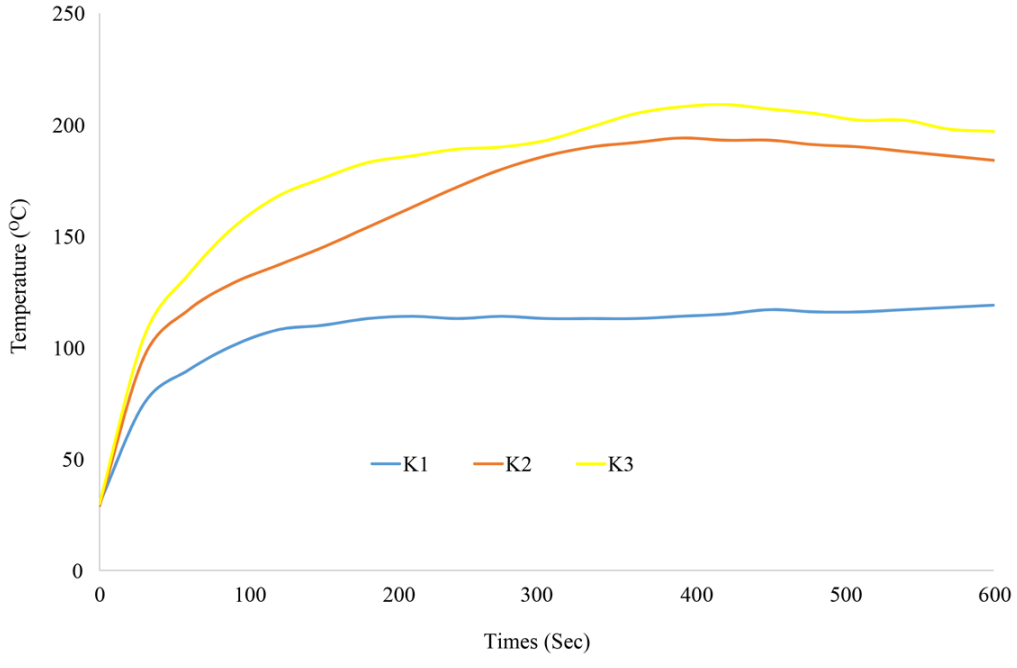

Fig. 10. Coffee bean temperature profile throughout the roasting process

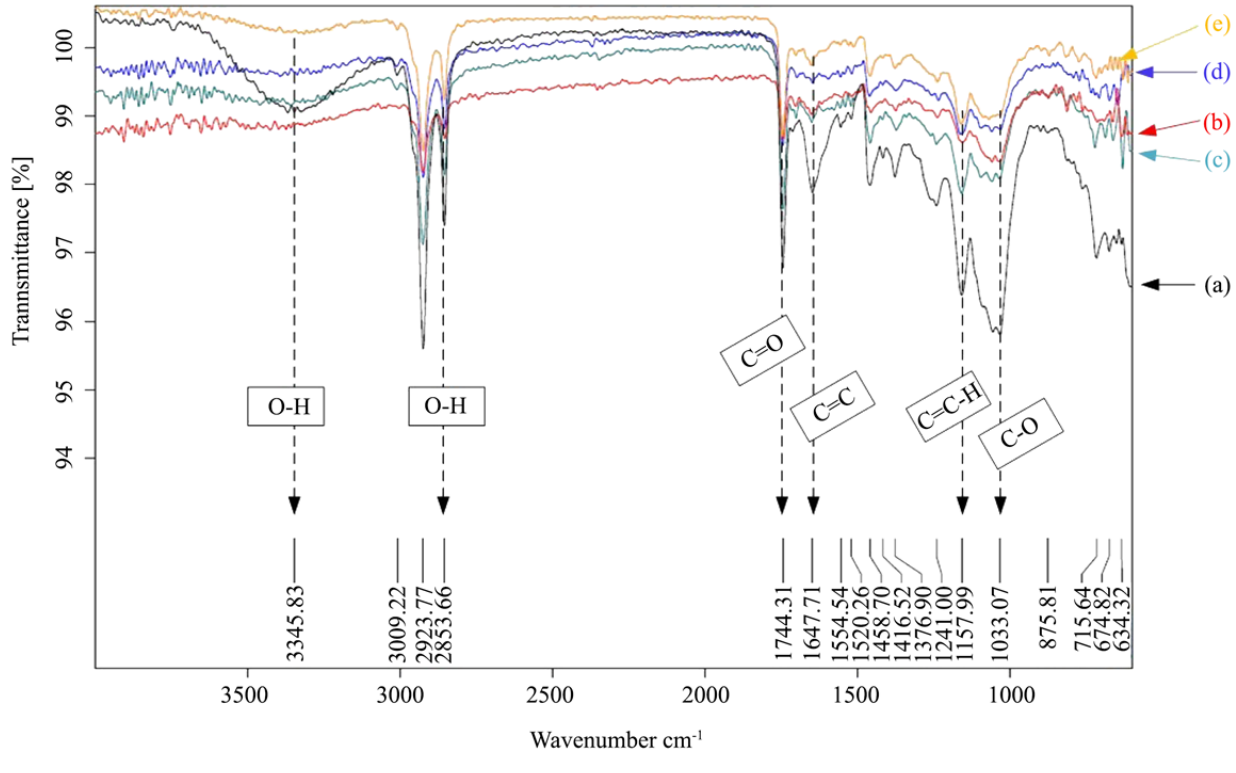

Fig. 11. FTIR spectrum of coffee beans: *a* — Green beans; *b* — Roasted coffee products with P_1 catalyst; *c* — Roasted coffee products with P_2 catalyst; *d* — Roasted coffee products with P_3 catalysts; and *e* — Conventionally roasted coffee products

The moisture content of the roasted coffee beans implies the role of catalyst surface area in content decomposition. Fig. 13 shows the change in water content from 12 % in green coffee beans (GB) to 7.08 % in coffee roasted with P_1 catalyst indicated by K_1 to 5.96 %, in coffee roasted with P_2 catalyst indicated by K_2 and to 5.44 % and, in coffee roasted with P_3 catalyst indicated by K_3. These indicates the coffee beans were shrinking due to the water evaporation.

The change in temperature profile may link to the final moisture content of the coffee product. Therefore, it is suggested that the different final moisture content was due to the different evaporation rate. The K_3 shows the performance of the P_3 catalyst in reducing the amount of water vapor in the material. Hence, the smaller surface area grains which indicated by high porosity were drastically reduce liquid composition of coffee beans.

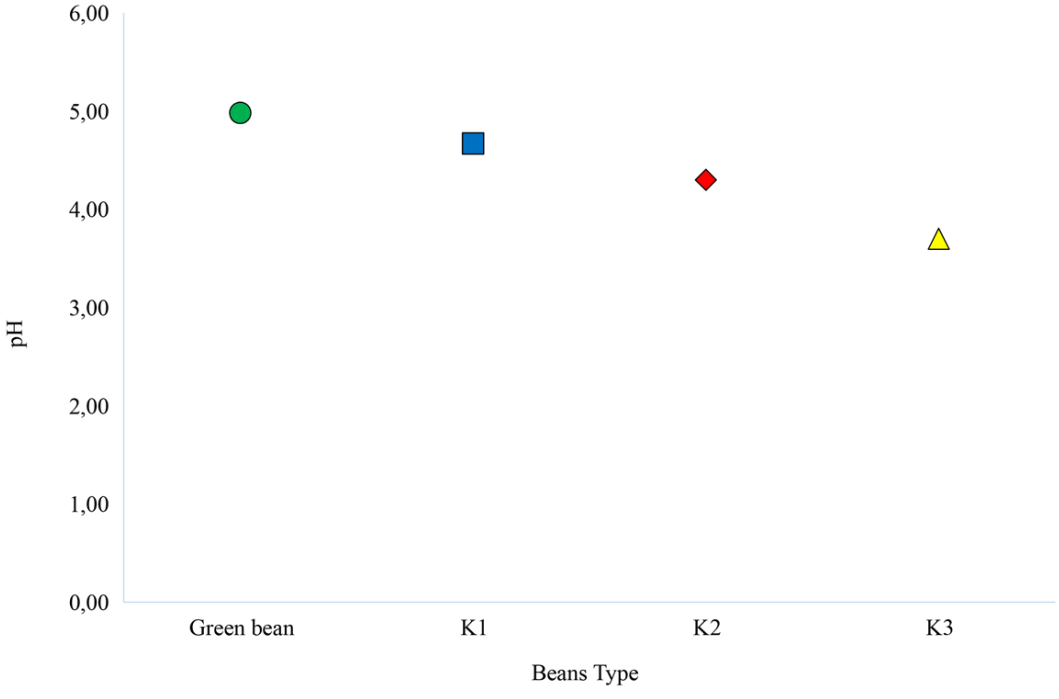

Fig. 12. Acidity level comparison between green coffee and each roasted coffee product with each pottery catalyst

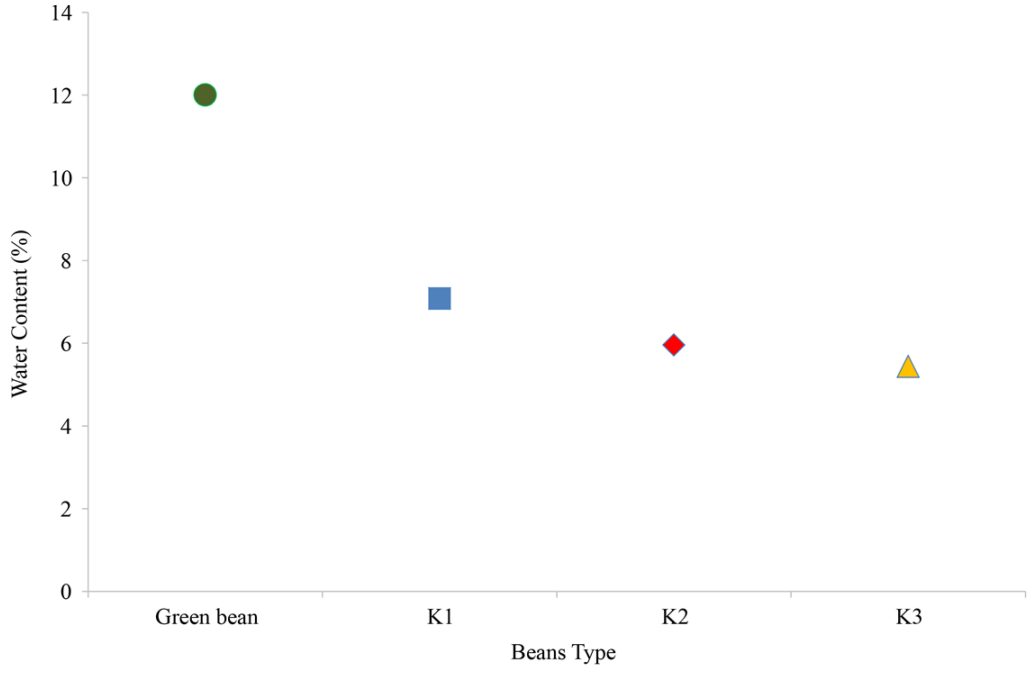

Fig. 13. Comparison of water content between green coffee and each coffee product roasted with a pottery catalyst

6. Discussion of experimental results

The dislocated electrons in the catalyst pores cannot absorb energy properly because the surface is covered with positive charges from impurity cations so that the contact area gets smaller. The heating process until reaching the critical temperature of clay will cause the clay surface to emit photons. The electrons interaction with photons around the pore was following the QED principle. Hence the surface electrons will jump from the valence band to the conduction band which shifts the pore polarity to be negative. The presence of the pore promotes charge gradient [41]. The charge gradient was due to the uncharged pore hole that dissecting charged surface around the hole. Therefore, the impurity cations are far enough to attract negative charge around the pores. As a result, the surface structure with low porosity weakens the hydrogen absorption capability. This condition was characterized by a modest increase in seed temperature as shown in Fig. 10 (K1). As the electron kinetic energy greatly influenced by temperature, this phenomenon slow down the decomposition rate.

The difference in grain temperature was caused by the increase in the conductivity of the catalyst. In the case of K2 and K3 coffee beans, the peak temperature can be reached

faster, namely 360 sec and 330 sec, respectively. The pottery catalysts P2 and P3 have a higher percentage of porosity which makes them have a more dominant charge gradient. Porous pottery catalyst with amorphous surface capable of generating an electric field when receiving light energy due to the heating process. As the heating process trigger the electrons around the pores to vibrate, the resulting photons give some energy to lift the electrons from valence band to the conduction band. As a result, the surface becomes conductive due to its high electron density. The highly populated electrons on the surface have generating segregated conductive area. The segregation was due to the existence of grain boundaries. However, the grain boundaries itself help to increase surface area of the catalyst grain. The edge of the grain boundaries also can be involved in the reaction. The edge of the ceramic grain boundaries were negatively charged ionic compound. The pores also contain negatively charge edges as the grain boundaries. Hence, the segregated electron dense region, the grain edges, and the pore edges are responsible for the adsorption strength of the pottery catalyst on the CGA molecules.

The fewer edges catalysts were unable to effectively reacting with CGA. The pottery catalysts utilize its conductivity to decompose CGA. Some amount of CGA molecules were decomposed naturally by heat. Although, the decomposition may imperfect due to the nature of the heat as the phonon vibration [42]. Also, the dipole moment induces by heat that has no acceptors will regain back as irregularities in the crystal if the crystal itself not closely packed [43]. In the case of ceramics, the cubical crystal lattices were compact and closely pack without the presence of impurities. Hence, the natural heating without catalysts not ensures the controlled decomposition rate of the CGA. The polar surface of pottery catalysts were acts as the dipole moment acceptor when the molecules were heated. Therefore, the CGA dipole moment will be accepted by the catalysts surface. The reaction mechanism has been illustrated in Fig. 14. One of the products of this interaction is the release of hydroxyl ions (OH^-) from the CGA. As the interaction continued, some of the hydroxyl ions were interacting with the catalyst surface. The result of the second interaction is hydrogen atoms (H2).

The porosity of P2 and P3 catalysts surface has given a lower resistance value of charge transport and triggers a faster interfacial charge transfer. The energy difference in each pottery catalyst (P1, P2 and P3) affects the rate of decomposition of coffee beans. The conductive surface of the pottery catalysts increases its electrical conductivity. So that the catalyst responsive to the energy received from the surrounding heat and converts it into electrical energy. The existence of pores decelerates the temperature gradient formation on the surface [44]. However, the heat that concentrated on smaller surface area may energize the pottery clay ionic edges. As a consequence, the decomposition reaction runs faster indicated by moisture content reduction rate.

The phenomenon of adsorption of hydroxyl and carbonyl groups in CGA is triggered by the negative charge of electrons in the pores of the catalyst. The polarity of the CGA adsorbed by the pores of the pottery catalyst has an important role that affects its interaction with the electric field of the catalyst. In general, clay-based pottery has a relatively large pore structure with an orthorhombic crystal structure and affects its function due to the mono-dimensional and non-intersectional nature of the pore and canal structure. This structure can inhibit the entry of large molecules. So that the Si/Al ratio of pottery can be increased by an activation process as an alternative to modify the structure, pores and area to reach the optimum Si/Al ratio as a catalyst [45]. Besides that, the grain size of the pottery catalyst affects the CGA adsorption process, where during the adsorption process it is necessary to contact the counter ion with the ionic group bound to the catalyst. The smaller the grain size, the larger the surface area. The large surface area makes the ionic groups are more exposed. As a result, the surface capacity of the catalyst will be increased due to the more attainable reaction sites.

The Si/Al ratio has the key role to enhance each catalyst heat and electrical conduction properties. Through Fig. 5 it can be clearly seen that the performance of P2 and P3 catalysts which have smaller grain size and high Si/Al ratios have given conductive large surface area sites. The surface area formed gives the effect of increasing the charged sites on the catalyst surface. When the catalyst temperature increases, $[AlO_4]^{5-}$ which is negatively charged will attract hydrogen to the carboxyl and hydroxyl groups stronger due to the energy of electrons that being dislocated in the pores. This surface interaction of the Si/Al catalyst consistent with the increase in the temperature of the coffee beans when roasted with P2 and P3 catalysts as illustrated in Fig. 10. The temperature profile of each catalysts roasting informs the kinetics of each catalyst.

Besides the type of the cations and the structure of the pottery catalyst framework, other factors affects the sorption properties of the material in the roasting process. The P1 with low Si/Al ratio causes the cation density and electrostatic field strength to be decreased and the affinity of the catalyst surface for non-polar groups in CGA to be increased as well reduce the polar group affinity. Catalysts that have higher alumina elements adsorb more water than hydrocarbons, but the opposite conditions will occur in catalysts containing higher silica. This due to the ability of aluminum atom to bond 6 water molecules as silicon only can bonds 4 water molecules. Where in Fig. 10, at the roasting time of 0–100 sec, the catalyst roasted coffee (K3) (P3) experienced a significant increase in temperature. In this hydration phase the catalyst (P3) with a Si/Al ratio attracting a lot of water molecules due to the presence of alumina. Aluminum atom has strength to poisoning active metal in a metal complex [46]. The balance ratio of zinc with aluminum in a Zn-Al anion intercalation matrix for double layer hydroxide increases surface adsorption capability [47]. The high concentration of alumina in the catalyst alters the magnetic properties of the pottery catalyst. The exposure of external magnetic field to the water molecule triggers the dipole homogenization [48]. Therefore, strong magnetic field will enforce the water molecules to move in the same direction. Consequently, the heat diffusion on each catalyst particle was different. Simultaneously, the translational motion of enforced water molecules will increase the evaporation rate of the material and have a significant effect on the decrease in water content as shown in Fig. 13.

A limitation that imposed in this study was the possibility of biased in surface charge analysis through SEM images surface brightness plot. This technique requires the flat sample surface in high vacuum SEM mode. Therefore, a contour difference will cause the result to be inaccurate. Still, the results have the consistency with the mineral content that obtained by EDX characterization. Consequently, the error of the surface charge analysis has not lead to the erroneous

conclusion. Alongside to that, the future problem that has to be tackled from this study is the development of controllable pottery catalyst. The decomposition control is needed because the CGA content is the main antioxidant of coffee that has many positive effects for human health. Also, further investigation of coffee protein with roaster minerals interaction is needed as the protein-mineral interaction affects nutritional content [49]. Thus, the decomposition ratio control to optimize coffee products quality while keeping the CGA content is important.

Some difficulties also present during understanding the maximization of coffee acidity due to the alumino-silicate ratio. The existence of various acids in coffee content such as palmitic acid, linoleic acid, and other acids may have different kind of acid taste. Therefore, the confirmation through pH value detection is utterly limited to show the increase in aliphatic acid without sensory evaluation. However, sensory evaluation also may differ due to various factors such as ethnical background, subjective preferences, and sensitivity. According to that, further analysis of coffee oil content during roasting may improve the accuracy of CGA decomposition results in objective manner.

7. Conclusions

1. The pottery with higher Si-Al ratio reach the peak roasting temperature faster due to the increased porosity. The porous have larger surface reaction area with fewer atomic bonds. Therefore, the higher porosity pottery heated faster.

2. The crystal defects, Si-Al ratio, and mineral content (Fe, Ti, etc.) have affecting heat to electricity conversion during the roasting process. The pottery catalyst contains amorphous alumino-silicate structure in different ratio depending to the activation treatment. The FTIR spectrum has shown the level of Si-O-Al surface absorption which is associated with the surface properties of the pottery catalyst.

3. The High Si-Al ratio of a pottery causes GB macronutrient molecules decomposition to form aliphatic acid which alter the cation transfer capability on the catalyst surface that indicated by the heat transmittance of the catalyst and increase the coffee product acidity indicated by lower pH value.

Conflict of interest

The authors declare that they have no conflict of interest in relation to this research, whether financial, personal, authorship or otherwise, that could affect the research and its results presented in this paper.

Acknowledgments

The author would like to thank the Department of Mechanical Engineering, Brawijaya University & PGRI Banyuwangi University for their encouragements and support.

References

1. Noor Aliah, A. M., Fareez Edzuan, A. M., Noor Diana, A. M. (2015). A Review of Quality Coffee Roasting Degree Evaluation. Journal of Applied Science and Agriculture, 10 (7), 18–23. Available at: https://www.researchgate.net/publication/280627747_A_Review_of_Quality_Coffee_Roasting_Degree_Evaluation
2. De Toledo, P. R. A. B., de Melo, M. M. R., Pezza, H. R., Toci, A. T., Pezza, L., Silva, C. M. (2017). Discriminant analysis for unveiling the origin of roasted coffee samples: A tool for quality control of coffee related products. Food Control, 73, 164–174. doi: https://doi.org/10.1016/j.foodcont.2016.08.001
3. Higdon, J. V., Frei, B. (2006). Coffee and Health: A Review of Recent Human Research. Critical Reviews in Food Science and Nutrition, 46 (2), 101–123. doi: https://doi.org/10.1080/10408390500400009
4. Tajik, N., Tajik, M., Mack, I., Enck, P. (2017). The potential effects of chlorogenic acid, the main phenolic components in coffee, on health: a comprehensive review of the literature. European Journal of Nutrition, 56 (7), 2215–2244. doi: https://doi.org/10.1007/s00394-017-1379-1
5. Uman, E., Colonna-Dashwood, M., Colonna-Dashwood, L., Perger, M., Klatt, C., Leighton, S. et. al. (2016). The effect of bean origin and temperature on grinding roasted coffee. Scientific Reports, 6 (1). doi: https://doi.org/10.1038/srep24483
6. Fareez Edzuan, A. M., Noor Aliah, A. M., Bong, H. L. (2015). Physical and Chemical Property Changes of Coffee Beans during Roasting. American Journal of Chemistry, 5 (3A), 56–60. Available at: http://article.sapub.org/10.5923.c.chemistry.201501.09.html
7. Belay, A., Gholap, A. V. (2009). Characterization and determination of chlorogenic acids (CGA) in coffee beans by UV-Vis spectroscopy. African Journal of Pure and Applied Chemistry, 3 (11), 234–240. Available at: https://academicjournals.org/journal/AJPAC/article-full-text-pdf/0E5B4BA1938
8. Çakır, S., Biçer, E., Yılmaz Arslan, E. (2015). A Newly Developed Electrocatalytic Oxidation and Voltammetric Determination of Curcumin at the Surface of PdNp-graphite Electrode by an Aqueous Solution Process with Al3+. Croatica Chemica Acta, 88 (2), 105–112. doi: https://doi.org/10.5562/cca2527
9. Šeruga, M., Tomac, I. (2014). Electrochemical behaviour of some chlorogenic acids and their characterization in coffee by square-wave voltammetry. International Journal of Electrochemical Science, 9 (11), 6134–6154. Available at: https://www.researchgate.net/publication/266494182_Electrochemical_Behaviour_of_Some_Chlorogenic_Acids_and_Their_Characterization_in_Coffee_by_Square-Wave_Voltammetry
10. Maggetti, M. (1982). Phase analysis and its significance for technology and origin. Smithsonian Institution Press. Available at: https://www.academia.edu/40783239/Phase_Analysis_and_its_Significance_for_Technology_and_Origin
11. Yang, C., Hu, C., Xiang, C., Nie, H., Gu, X., Xie, L. et. al. (2021). Interfacial superstructures and chemical bonding transitions at metal-ceramic interfaces. Science Advances, 7 (11). doi: https://doi.org/10.1126/sciadv.abf6667

12. Ion, R.-M., Fierascu, R.-C., Teodorescu, S., Fierascu, I., Bunghez, I.-R., Turcanu-Carutiu, D., Ion, M.-L. (2016). Ceramic Materials Based on Clay Minerals in Cultural Heritage Study. Clays, Clay Minerals and Ceramic Materials Based on Clay Minerals. doi: https://doi.org/10.5772/61633
13. Sposito, G., Sommers, L. E. (1985). Chemical models of inorganic pollutants in soils. Critical Reviews in Environmental Control, 15 (1), 1–24. doi: https://doi.org/10.1080/10643388509381725
14. Melar, J., Bednarik, V., Slavik, R., Pastorek, M. (2013). Effect of hydrothermal treatment on the structure of an aluminosilicate polymer. Open Chemistry, 11 (5), 782–789. doi: https://doi.org/10.2478/s11532-013-0204-9
15. Geraldo, R. H., Camarini, G. (2015). Geopolymers Studies in Brazil: A Meta-Analysis and Perspectives. International Journal of Engineering and Technology, 7 (5), 390–396. doi: https://doi.org/10.7763/ijet.2015.v7.825
16. Bhatt, K. N., Halligudi, S. B. (1994). Hydroformylation of allyl alcohol catalysed by (Rh(PPh3)3)+/montmorillonite: A kinetic study. Journal of Molecular Catalysis, 91 (2), 187–194. doi: https://doi.org/10.1016/0304-5102(94)00036-0
17. Münchow, M., Alstrup, J., Steen, I., Giacalone, D. (2020). Roasting Conditions and Coffee Flavor: A Multi-Study Empirical Investigation. Beverages, 6 (2), 29. doi: https://doi.org/10.3390/beverages6020029
18. Dias, R., Benassi, M. (2015). Discrimination between Arabica and Robusta Coffees Using Hydrosoluble Compounds: Is the Efficiency of the Parameters Dependent on the Roast Degree? Beverages, 1 (3), 127–139. doi: https://doi.org/10.3390/beverages1030127
19. Alstrup, J., Petersen, M. A., Larsen, F. H., Münchow, M. (2020). The Effect of Roast Development Time Modulations on the Sensory Profile and Chemical Composition of the Coffee Brew as Measured by NMR and DHS-GC–MS. Beverages, 6 (4), 70. doi: https://doi.org/10.3390/beverages6040070
20. Yang, N., Liu, C., Liu, X., Degn, T. K., Munchow, M., Fisk, I. (2016). Determination of volatile marker compounds of common coffee roast defects. Food Chemistry, 211, 206–214. doi: https://doi.org/10.1016/j.foodchem.2016.04.124
21. Rostagno, M. A., Celeghini, R. M. S., Debien, I. C. N., Nogueira, G. C., Meireles, M. A. A. (2015). Phenolic Compounds in Coffee Compared to Other Beverages. Coffee in Health and Disease Prevention, 137–142. doi: https://doi.org/10.1016/b978-0-12-409517-5.00015-2
22. Yeager, S. E., Batali, M. E., Guinard, J.-X., Ristenpart, W. D. (2021). Acids in coffee: A review of sensory measurements and meta-analysis of chemical composition. Critical Reviews in Food Science and Nutrition, 1–27. doi: https://doi.org/10.1080/10408398.2021.1957767
23. Saeed Alkaltham, M., Musa Özcan, M., Uslu, N., Salamatullah, A. M., Hayat, K. (2020). Effect of microwave and oven roasting methods on total phenol, antioxidant activity, phenolic compounds, and fatty acid compositions of coffee beans. Journal of Food Processing and Preservation, 44 (11). doi: https://doi.org/10.1111/jfpp.14874
24. Mohorič, T., Bren, U. (2020). How does microwave irradiation affect the mechanism of water reorientation? Journal of Molecular Liquids, 302, 112522. doi: https://doi.org/10.1016/j.molliq.2020.112522
25. Mitsudo, S., Sako, K., Tani, S., Sudiana, I. N. (2011). High power pulsed submillimeter wave sintering of zirconia ceramics. 2011 International Conference on Infrared, Millimeter, and Terahertz Waves. doi: https://doi.org/10.1109/irmmw-thz.2011.6105135
26. Gordienko, P. S., Shabalin, I. A., Yarusova, S. B., Slobodyuk, A. B., Somova, S. N. (2017). Composition, structure, and morphology of nanostructured aluminosilicates. Theoretical Foundations of Chemical Engineering, 51 (5), 763–768. doi: https://doi.org/10.1134/s0040579517050104
27. Cui, X.-M., Zheng, G.-J., Han, Y.-C., Su, F., Zhou, J. (2008). A study on electrical conductivity of chemosynthetic Al_2O_3–$2SiO_2$ geoploymer materials. Journal of Power Sources, 184 (2), 652–656. doi: https://doi.org/10.1016/j.jpowsour.2008.03.021
28. Suryanarayana, C. (2004). Mechanical Alloying And Milling. CRC Press, 488. doi: https://doi.org/10.1201/9780203020647
29. Konar, D., Bhattacharyya, S., Panigrahi, B. K., Ghose, M. K. (2017). An efficient pure color image denoising using quantum parallel bidirectional self-organizing neural network architecture. Quantum Inspired Computational Intelligence, 149–205. doi: https://doi.org/10.1016/b978-0-12-804409-4.00005-x
30. Basavaraj, K., Gopinandhan, T. N., Gupta, N., Banakar, M. (2014). Relationship between Sensory Perceived Acidity and Instrumentally Measured Acidity in Indian Coffee Samples. J. Nutr. Diet., 51, 286. doi: https://doi.org/10.13140/RG.2.2.29177.52328
31. Al-Sehemi, A. G., Al-Ghamdi, A. A., Dishovsky, N., Nickolov, R. N., Atanasov, N. T., Manoilova, L. T. (2017). Effect of Activated Carbons on the Dielectric and Microwave Properties of Natural Rubber Based Composites. Materials Research, 20 (5), 1211–1220. doi: https://doi.org/10.1590/1980-5373-mr-2017-0378
32. Belver, C., Bañares Muñoz, M. A., Vicente, M. A. (2002). Chemical Activation of a Kaolinite under Acid and Alkaline Conditions. Chemistry of Materials, 14 (5), 2033–2043. doi: https://doi.org/10.1021/cm0111736
33. Ungár, T. (2004). Microstructural parameters from X-ray diffraction peak broadening. Scripta Materialia, 51 (8), 777–781. doi: https://doi.org/10.1016/j.scriptamat.2004.05.007
34. Khatamian, M., Irani, M. (2009). Preparation and characterization of nanosized ZSM-5 zeolite using kaolin and investigation of kaolin content, crystallization time and temperature changes on the size and crystallinity of products. Journal of the Iranian Chemical Society, 6 (1), 187–194. doi: https://doi.org/10.1007/bf03246519
35. Postek, M. T., Vladár, A. E. (2015). Does your SEM really tell the truth? How would you know? Part 4: Charging and its mitigation. Scanning Microscopies 2015. doi: https://doi.org/10.1117/12.2195344
36. Funabashi, H., Takeuchi, S., Tsujimura, S. (2017). Hierarchical meso/macro-porous carbon fabricated from dual MgO templates for direct electron transfer enzymatic electrodes. Scientific Reports, 7 (1). doi: https://doi.org/10.1038/srep45147

37. Kaur, P., Park, Y., Sillanpää, M., Imteaz, M. A. (2021). Synthesis of a novel SnO_2/graphene-like carbon/TiO_2 electrodes for the degradation of recalcitrant emergent pharmaceutical pollutants in a photo-electrocatalytic system. Journal of Cleaner Production, 313, 127915. doi: https://doi.org/10.1016/j.jclepro.2021.127915
38. Narodny, L., Feynman, R. (1991). QED: The Strange Theory of Light and Matter. Leonardo, 24 (4), 493. doi: https://doi.org/10.2307/1575549
39. Purnami, Hamidi, N., Sasongko, M. N., Widhiyanuriyawan, D., Wardana, I. N. G. (2020). Strengthening external magnetic fields with activated carbon graphene for increasing hydrogen production in water electrolysis. International Journal of Hydrogen Energy, 45 (38), 19370–19380. doi: https://doi.org/10.1016/j.ijhydene.2020.05.148
40. Willy Satrio, N., Winarto, Sugiono, Wardana, I. N. G. (2020). Hydrogen production from instant noodle wastewater by organic electrocatalyst coated on PVC surface. International Journal of Hydrogen Energy, 45 (23), 12859–12873. doi: https://doi.org/10.1016/j.ijhydene.2020.03.002
41. Satrio, N. W., Winarto, Sugiono, Wardana, I. N. G. (2020). The role of turmeric and bicnat on hydrogen production in porous tofu waste suspension electrolysis. Biomass Conversion and Biorefinery, 12 (7), 2417–2429. doi: https://doi.org/10.1007/s13399-020-00803-0
42. Wright, A. D., Verdi, C., Milot, R. L., Eperon, G. E., Pérez-Osorio, M. A., Snaith, H. J. et. al. (2016). Electron–phonon coupling in hybrid lead halide perovskites. Nature Communications, 7 (1). doi: https://doi.org/10.1038/ncomms11755
43. Melloni, A., Rossi Paccani, R., Donati, D., Zanirato, V., Sinicropi, A., Parisi, M. L. et. al. (2010). Modeling, Preparation, and Characterization of a Dipole Moment Switch Driven by Z/E Photoisomerization. Journal of the American Chemical Society, 132 (27), 9310–9319. doi: https://doi.org/10.1021/ja906733q
44. Siswanto, E., Rifan, A. Z., Purnami, Widhiyanuriyawan, D., Darmadi, D. B. (2019). The Effect of Porosity on The Temperature Spectrum Area and Heat Transfer in Chamber with Porous Media Under the Saturated Vapour Flow. IOP Conference Series: Materials Science and Engineering, 494, 012071. doi: https://doi.org/10.1088/1757-899x/494/1/012071
45. Fernandes, L. D., Bartl, P. E., Monteiro, J. F., da Silva, J. G., de Menezes, S. C., Cardoso, M. J. B. (1994). The effect of cyclic dealumination of mordenite on its physicochemical and catalytic properties. Zeolites, 14 (7), 533–540. doi: https://doi.org/10.1016/0144-2449(94)90187-2
46. Kotok, V., Kovalenko, V. (2017). Electrochromism of $Ni(OH)_2$ films obtained by cathode template method with addition of Al, Zn, Co ions. Eastern-European Journal of Enterprise Technologies, 3 (12 (87)), 38–43. doi: https://doi.org/10.15587/1729-4061.2017.103010
47. Kovalenko, V., Borysenko, A., Kotok, V., Nafeev, R., Verbitskiy, V., Melnyk, O. (2022). Determination of the dependence of the structure of Zn-Al layered double hydroxides, as a matrix for functional anions intercalation, on synthesis conditions. Eastern-European Journal of Enterprise Technologies, 1 (12 (115)), 12–20. doi: https://doi.org/10.15587/1729-4061.2022.252738
48. Purnami, P., Hamidi, N., Nur Sasongko, M., Siswanto, E., Widhiyanuriyawan, D., Pambudi Tama, I. et. al. (2022). Enhancement of hydrogen production using dynamic magnetic field through water electrolysis. International Journal of Energy Research, 46 (6), 7309–7319. doi: https://doi.org/10.1002/er.7638
49. Serik, M., Samokhvalova, O., Kholobtseva, I., Fedak, N., Bolkhovitina, O., Sova, N., Chornei, K. (2021). Determining the influence of protein-mineral additives on the properties of butter cookies emulsion. Eastern-European Journal of Enterprise Technologies, 4 (11 (112)), 42–49. doi: https://doi.org/10.15587/1729-4061.2021.237890